



Research article

Modelling MR and clinical features in grade II/III astrocytomas to predict IDH mutation status



Harpreet Hyare^{a,b,*}, Louise Rice^c, Stefanie Thust^{a,c}, Parashkev Nachev^a, Ashwani Jha^a, Marina Milic^c, Sebastian Brandner^{d,e}, Jeremy Rees^{a,c}

^a Department of Brain Repair and Rehabilitation, UCL Institute of Neurology, London, UK

^b Imaging Department, UCLH NHS Trust, London, UK

^c National Hospital for Neurology and Neurosurgery, Queen Square, London, UK

^d Division of Neuropathology, National Hospital for Neurology and Neurosurgery, Queen Square, London, UK

^e Department of Neurodegenerative Diseases, UCL Institute of Neurology, London, UK

ARTICLE INFO

Keywords:

MRI
VASARI
IDH
Astrocytoma

ABSTRACT

Background and purpose: There is increasing evidence that many IDH wildtype (IDHwt) astrocytomas have a poor prognosis and although MR features have been identified, there remains diagnostic uncertainty in the clinic. We have therefore conducted a comprehensive analysis of conventional MR features of IDHwt astrocytomas and performed a Bayesian logistic regression model to identify critical radiological and basic clinical features that can predict IDH mutation status.

Materials and methods: 146 patients comprising 52 IDHwt astrocytomas (19 WHO Grade II diffuse astrocytomas (A II) and 33 WHO Grade III anaplastic astrocytomas (A III)), 68 IDHmut astrocytomas (53 A II and 15 A III) and 26 GBM were studied. Age, sex, presenting symptoms and Overall Survival were recorded. Two neuroradiologists assessed 23 VASARI imaging descriptors of MRI features and the relation between IDH mutation status and MR and basic clinical features was modelled by Bayesian logistic regression, and survival by Kaplan-Meier plots. **Results:** The features of greatest predictive power for IDH mutation status were, age at presentation (OR = 0.94 +/−0.03), tumour location within the thalamus (OR = 0.15 +/−0.25), involvement of speech receptive areas (OR = 0.21 +/−0.26), deep white matter invasion of the brainstem (OR = 0.10 +/−0.32), and T1/FLAIR signal ratio (OR = 1.63 +/−0.64). A logistic regression model based on these five features demonstrated excellent out-of-sample predictive performance (AUC = 0.92 +/−0.07; balanced accuracy 0.81 +/−0.09). Stepwise addition of further VASARI variables did not improve performance.

Conclusion: Five demographic and VASARI features enable excellent individual prediction of IDH mutation status, opening the way to identifying patients with IDHwt astrocytomas for earlier tissue diagnosis and more aggressive management.

Summary of importance

This study adds to existing evidence by highlighting the significantly worse prognosis of low to intermediate grade IDH wildtype (IDHwt) astrocytomas compared to their IDH mutant (IDHmut) counterparts, with a striking similarity in Overall Survival (OS) between WHO III IDHwt and GBM, demonstrating the significant effect of WHO tumour grade. IDHwt astrocytomas are suspected to represent 'early GBM' making it vital to identify these patients for early and aggressive treatment. From a comprehensive analysis of structural MR imaging in IDHwt grade II and grade III astrocytomas, we identify five critical imaging and demographic features with substantial power to predict

IDH mutation status. The current strategy of 'imaging only' observational management for gliomas of presumed low grade, without diagnostic biopsy, may thus be modified by probabilistically stratified risk of adverse tumour genetics.

1. Introduction

The recently published World Health Organization Classification of tumours [1] has now incorporated molecular parameters to complement histological features in the definition of tumour entities. In the updated WHO guidelines, WHO grade II diffuse astrocytomas (A II) and WHO grade III anaplastic astrocytomas (A III) are now divided into IDH

* Corresponding author at: Department of Brain Repair and Rehabilitation, UCL Institute of Neurology, Queen Square, London, WC1N 3BG, UK.

E-mail address: harpreet.hyare@nhs.net (H. Hyare).

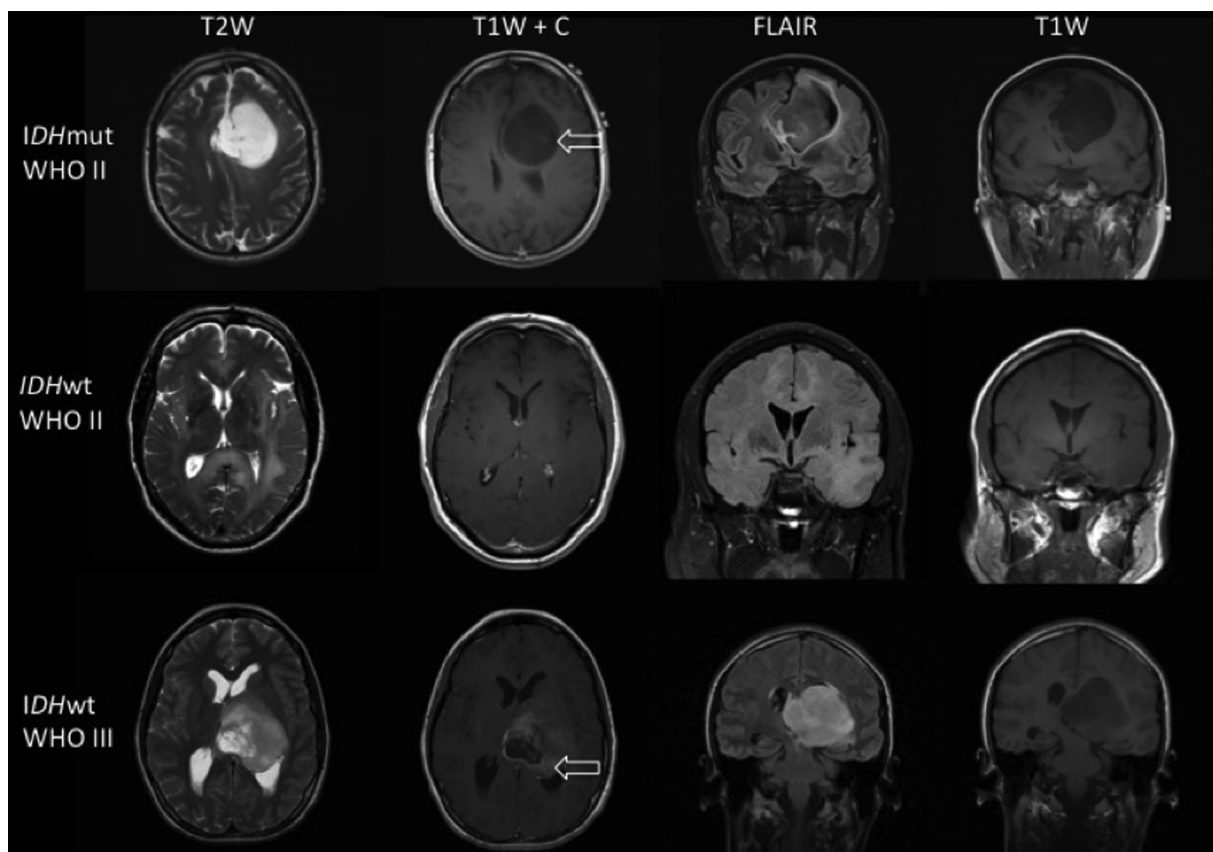


Fig. 1. Illustration of effect of IDH mutation status on VASARI MRI features. legend: *IDHmut* WHO grade II tumour in left frontal lobe demonstrating a well-defined nonenhancing margin on T2W, patchy enhancement on T1W + C and T1 FLAIR ratio. *IDHwt* WHO grade II tumour centred on the left temporal lobe, demonstrating a poorly-defined non enhancing margin with gliomatosis on T2W, no contrast enhancement on T1W + C and T1 < < FLAIR ratio. *IDHwt* WHO grade III thalamic tumour demonstrating a well-defined tumour margin on T2W, thick/nodular enhancement > 3mm on T1W + C and T1 FLAIR ratio.

mutant (*IDHmut*), *IDH* wildtype (*IDHwt*) and not otherwise specified (NOS) categories. A recent study of more than 160 adult *IDHwt* astrocytomas demonstrated that 78% were the molecular equivalent of conventional glioblastoma (GBM) based on molecular profiles and hallmark DNA alterations with similar poor survival profiles [2].

There are now numerous reports predicting *IDH* mutation status using both conventional and quantitative MRI. *IDHwt* tumours have been shown to have an indistinct tumour margin [3], tend to involve the temporal lobes, demonstrate lower ADC and have a higher rCBV [4] compared to *IDHmut* tumours. Whilst these findings are important, in isolation these MR features are non-specific, leading to diagnostic uncertainty.

At our institution, we have also observed that a number of patients with histology suggestive of astrocytoma WHO grade II or III, but molecular features of primary glioblastoma, including *IDHwt*, 7p gain or EGFR amplification, 10q loss and TERT promoter mutation, have behaved clinically similar to GBM. The purpose of this study was to identify a robust set of clinical and radiological features that could accurately identify this group of 'early stage GBM'.

We performed a comprehensive qualitative imaging analysis of *IDHwt* astrocytomas using the VASARI (Visually Accessible Rembrandt Images) MR feature set [5] and compared with two reference sets of *IDHmut* astrocytomas and GBM. A Bayesian logistic regression model was then used to identify the critical MR and demographic features with substantial power to predict IDH mutation status.

2. Materials and methods

2.1. Patient population

146 consecutive patients undergoing surgery were selected from the archives of the Neuropathology Department at our Institution between 2012 and 2017, following appropriate institutional review board approval. They comprised 52 *IDHwt* astrocytomas (19 A II and 33 A III), 68 *IDHmut* astrocytomas (53 A II and 15 A III) and 26 *IDHwt* GBM.

Clinical information (age, sex) and overall survival was available in all cases and presenting symptom was available in all WHO grade II/III astrocytoma cases. Overall survival was defined as the number of months between the date of the initial pathological diagnosis and time to death (or point of censure if patient was still alive). In addition, the proportion of patients still alive at two years was determined in each group. Pre-surgical MRI data were available in all cases, of which contrast images were not available in 4 cases (3 *IDHmut*, 1 *IDHwt*) fluid attenuated inversion recovery (FLAIR) images were not available in 6 patients (2 *IDHwt*, 4 *IDHmut*), ADC maps were not available in 18 patients (7 *IDHwt* and 11 *IDHmut*) and the presence of haemorrhage could not be determined in 35 patients (12 *IDHwt* and 23 *IDHmut*).

2.2. Radiological features

The VASARI lexicon for MRI annotation contains 25 imaging descriptors based on different MRI modalities, including T1 and T2/FLAIR sequences, and was developed for use in analyzing GBMs. The exact description of all the features can be found at the National Cancer Institute's Cancer Imaging Archive (<https://wiki.cancerimagingarchive.net/display/Public/VASARI+Research+Project>).

For the purposes of this study, the most commonly used MRI features were assessed: f1 tumor location, f2 side of lesion center, f3 eloquent brain, f4 enhancement quality, f5 proportion enhancing, f6 proportion non-contrast enhancing tumor (nCET), f7 proportion necrosis, f8 cysts, f9 multifocal or multicentric, f10 T1/FLAIR ratio, f11 thickness of enhancing margin, f12 definition of the enhancing margin, f13 definition of the nonenhancing margin, f14 proportion of edema, f16 hemorrhage, f17 diffusion characteristics, f18 pial invasion, f19 ependymal invasion, f20 cortical involvement, f21 deep white matter invasion, f24 satellites, and f25 calvarial remodeling.

In a subset of 33 patients with *IDHwt* astrocytomas and 30 patients with *IDHmut* astrocytomas, two board-certified neuroradiologists (HH and ST) independently reviewed the MR images on a PACS workstation, blinded to histopathological diagnosis, and recorded a set of mark-ups for imaging features describing the location and morphology of the tumour. After initial review of this subset, modifications were made to some of the VASARI feature set to capture MRI features, which appeared unique to diffuse astrocytomas and anaplastic astrocytomas compared to GBMs. As a number of tumours demonstrated no contrast enhancement, an additional category “Not applicable” was added to f5 proportion enhancing, f11 thickness of enhancing margin and f12 definition of enhancing margin. In addition, an extra category “patchy” was added to f11 thickness of the enhancing margin to better describe the ill-defined enhancement perceived in many of the diffuse and anaplastic astrocytomas (Fig. 1).

The modified VASARI features were recorded on the remaining dataset by a clinical research fellow and checked by neuroradiologist HH.

2.3. Interrater agreement

We assessed the interrater agreement in the training set of each of the VASARI criteria by using the Kappa statistic. Values close to 1 indicate high interrater agreement for that particular feature, whereas values close to 0 signify that interrater agreement is due to chance. Interrater agreement for the lesion size measurements was assessed by means of the intraclass correlation coefficient. Finally, for each patient image set, a consensus review was performed for f4 enhancement quality, f11 thickness of enhancing margin, f12 definition of enhancing margin and f17 diffusion characteristics. For the remaining MR features, the consensus value was equal to the median of the neuroradiologists' measurements.

2.4. Histopathology and molecular analysis

Paraffin blocks containing tissue of adult patients (above 18 years) with *IDHwt* A II or A III were collected from the archives of the Neuropathology department at our Institution and analysed according to previously published data [6].

2.5. Association between MRI features and genomics

For descriptive purposes, a univariate analysis of the association of each of the 25 VASARI features with the clinical label was performed with a Chi-Squared test, uncorrected for multiple comparisons.

Independently, we sought to derive a multivariable statistical model that could be used to predict the genetic mutation status (*IDHwt* versus *IDHmut*) of grade II and grade III astrocytomas, based on a combination of basic clinical and radiological criteria. To achieve this, the genetic mutation status of 120 subjects with grade II/III astrocytomas (52 *IDHwt*, 68 *IDHmut*) was subjected to a Bayesian penalized logistic multiple regression model using the fully automated BayesReg software package (<https://arxiv.org/abs/1611.06649>), running in Matlab version 2016b (<https://uk.mathworks.com/>). Independent variables included age at presentation, gender, and the VASARI imaging descriptors. Each ordinal VASARI criterion (such as F10 T1/FLAIR ratio)

was modelled as a single covariate using dummy coding of the categorical levels. Nominal variables were parameterized with categorical expansion: for example F1 Tumour location is thereby decomposed into 8 categorical variables corresponding to each anatomical location. The following variables with fewer than 2 occurrences were removed from the dataset: F1 Tumour Location (Brainstem); F1 Tumour Location (Occipital Lobe); F3 Eloquent Brain (Vision); F11 Thickness of enhancing margin (Thin); F17 Diffusion (Restricted).

This reparameterisation resulted in a logistic multiple regression model with 50 independent variables. Where the number of independent variables is large relative to the number of cases in the data, estimating a model with conventional statistical methods can lead to extreme and unstable model parameters with high variance, resulting in poor out-of-sample predictive power. We therefore used penalised regression, applying a penalty to extreme model parameter estimates. In the Bayesian setting, this is robustly achieved by applying a shrinkage prior: a hyperparameter of the regression coefficients, whose distribution has a substantial mass around zero. Here we used the default ridge prior in the BayesReg package which is a half-Cauchy function with mean of zero and scale parameter of 1.

High-dimensional models are analytically intractable and so marginal likelihoods and posterior parameter estimates were estimated using Markov Chain Monte Carlo (MCMC) sampling using Gibbs procedure. The model was estimated from 50,000 samples (2000 samples burn-in and every 5th sample was included (thinning)). Odds ratios are presented as maximum a posteriori (MAP) estimates +/- standard deviation (sd).

Following estimation of the full model with the entire dataset, we investigated the predictive power of model with a reduced number of independent variables. For this stage, each regression coefficient was ranked according to a Bayesian feature ranking algorithm (Malik and Schmidt, 2011), where higher ranks indicate a stronger relationship between the dependent variable and the independent variable in question. We created 50 variants of the regression model, incrementally adding independent variables on order of their rank (from 1 variable up to 50 variables). The same MCMC settings were used as for the full model. In order to avoid overfitting, each model was estimated 100 times holding out 15% of the data and model performance was measured with out-of-sample predictive performance as quantified by the mean +/- sd of the area under the curve (AUC) of the Receiver operating characteristic (ROC) curve and mean +/- sd of the balanced accuracy.

Note an advantage of adopting a Bayesian framework is intelligibility of null results, allowing us to infer not only that a feature is associated but also that it is not.

3. Results

3.1. Interrater agreement

Interrater agreements were moderate to high. The highest agreement was seen for f1 tumour location (0.723) and f8 presence of tumour cyst(s) (0.713). The lowest agreement was for f17 diffusion characteristics (0.357) prior to consensus review.

3.2. Patient features and mutation status

Patients with *IDHwt* astrocytomas were significantly older than patients with *IDHmut* astrocytomas (mean 54 (21–76) years compared to 37 (20–63) years) and with GBM (mean age 42 (29–68) years (Table 1). No significant differences were observed for gender or presenting symptoms (Table 1). Seizure was the most common presenting symptom, seen in 39 of 68 *IDHmut* patients, 20 of 52 *IDHwt* patients and 12 of 26 GBM patients followed by motor paresis and dysphasia.

Table 1
Differences in VASARI MR features between the study set.

Variable	GBM (n=26)	IDHwt (n=52)	IDHmut (n=68)	IDHwt vs IDHmut	IDHwt vs GBM
Age (year)	42 (29–68)	54 (21–76)	37 (20–63)	< 0.001	0.274
Sex (male:female)	13:13	34:18	38:30	0.292	0.793
Presenting complaint				0.377	0.230
Cognitive disorder	2	5	3		
Dizziness	0	2	2		
Dysphasia	0	7	4		
Gait disturbance	2	1	1		
Headache	3	3	3		
Incidental	0	3	5		
Isolated CN	0	2	3		
Motor paresis	7	8	3		
Seizure	12	20	39		
Sensory disturbance	0	1	2		
Visual field disturbance	0	0	1		
F1 Tumour Location					
Cerebellum	0	1	0		
Corpus Callosum	0	2	1		
Frontal Lobe	11	13	37		
Insula	1	4	4	0.001	0.682
Occipital Lobe	1	1	0		
Parietal Lobe	4	5	8		
Temporal Lobe	6	15	18		
Thalamus	3	11	0		
F2 Side of lesion				0.235	0.681
Center/Bilateral	1	5	2		
Left	12	26	32		
Right	13	21	34		
F3 Eloquent Brain				0.007	0.726
Motor	4	8	8		
No Eloquent Brain	18	30	44		
Speech motor	0	3	13		
Speech receptive	3	11	2		
Vision	1	0	1		
F4 Enhancement Quality				0.663	0.003
Marked/avid	18	9	8		
Minimal/Mild	8	18	21		
No Contrast Enhancement	0	24	36		
No Contrast given	0	1	3		
F5 Proportion Enhancing				0.773	< 0.001
68-95%	6	1	1		
34-67%	6	7	5		
6-33%	13	16	21		
< 5%	1	3	2		
None	0	24	36		
N/A	0	1	3		
F6 Proportion Non-Contrast				0.538	< 0.001
68-95%	12	42	59		
34-67%	7	7	5		
6-33%	7	1	1		
< 5%	0	2	3		
F7 Proportion Necrosis				0.872	< 0.001
68-95%	1	0	0		
34-67%	8	4	3		
6-33%	10	3	5		
< 5%	2	1	1		
None	5	44	59		
F8 Cysts				0.022	0.176
Present	20	2	12		
Absent	6	50	56		
F9 Multifocal or Multicentric				0.005	0.190
Focal	23	32	58		
Gliomatosis	0	11	8		
Multifocal	3	9	2		
F10 T1/FLAIR ratio				< 0.001	0.002

Table 1 (continued)

Variable	GBM (n=26)	IDHwt (n=52)	IDHmut (n=68)	IDHwt vs IDHmut	IDHwt vs GBM
No FLAIR images	4	2	4		
T1 < FLAIR	4	27	9		
T1 < FLAIR	4	13	22		
T1~FLAIR	14	10	33		
F11 Thickness of enhancing margin				0.388	0.003
Patchy	4	13	20		
Solid	3	5	2		
Thick/nodular	15	7	4		
Thin	4	1	0		
Minimal	0	1	3		
N/A	0	25	39		
F12 Definition of the enhancing margin				0.138	0.011
Poorly defined	13	17	23		
Well defined	13	10	6		
N/A	0	25	39		
F13 Definition of the non-enhancing margin				< 0.001	0.162
Poorly defined	15	40	28		
Well defined	11	12	40		
F14 Proportion of Edema				0.160	0.003
34-67%	3	1	1		
6-33%	10	5	3		
< 5%	10	18	14		
None	3	28	50		
F16 Haemorrhage				0.434	0.375
Cannot determine	6	12	23		
No	15	37	42		
Yes	5	3	3		
F17 Diffusion Characteristics				0.713	0.001
No ADC Images	4	7	11		
Facilitated	4	27	37		
Mixed	14	18	19		
Restricted	4	0	1		
F18 Pial Invasion				0.232	0.023
Absent	20	51	63		
Present	6	1	5		
F19 Ependymal Extension				0.697	0.494
Absent	24	50	63		
Present	2	2	5		
F20 Cortical Involvement				0.034	0.109
Absent	10	15	8		
Present	16	37	60		
F21 Deep White Matter Invasion				< 0.001	0.916
Brainstem	1	6	0		
Corpus Callosum	3	9	10		
Internal Capsule	7	15	6		
None	15	22	52		
F24 Satellites				0.042	1.000
Absent	24	46	67		
Present	2	6	1		
F25 Calvarial Remodeling				0.315	1.000
Absent	24	49	67		
Present	2	3	1		

Note. GBM: glioblastoma, IDHwt: isocitrate dehydrogenase wild type, IDHmut: isocitrate dehydrogenase mutated, VASARI: Visually Accessible Rembrandt Images.

3.3. Patient survival

Overall Survival was available in 120 patients (13 GBM, 59 IDHmut and 48 IDHwt) and is shown by Kaplan-Meier plots for each tumour category in Fig. 2. As can be seen, the IDHwt A III and IDHwt A II

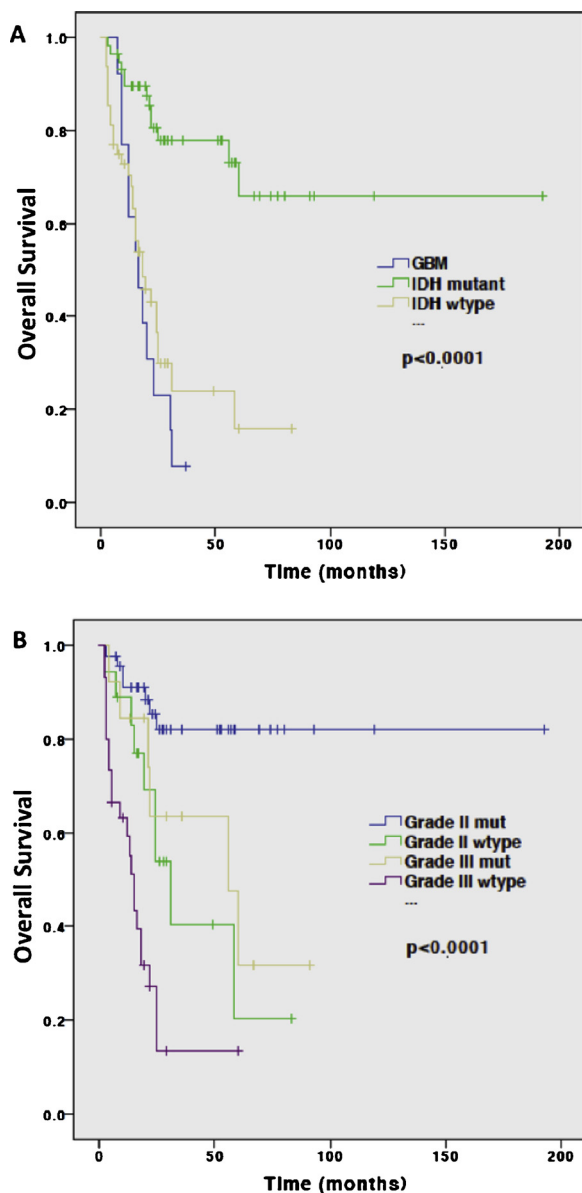


Fig. 2. Kaplan Meier survival curves illustrating effect of tumour grade and *IDH* mutation on Overall Survival. legend: Kaplan Meier survival curves demonstrating: (A) significantly poorer survival in *IDHwt* compared to *IDHmut* astrocytomas ($p < 0.0001$) but similar survival to GBM, (B) poorer survival in Grade III *IDHmut* astrocytomas compared to Grade II *IDHmut* ($p = 0.031$) and Grade III *IDHwt* compared to Grade II *IDHwt* astrocytomas ($p = 0.013$).

demonstrated poorer survival compared to the *IDHmut* reference set ($p < 0.001$) and, as expected, the GBM patients demonstrated the poorest overall survival. The median survival for *IDHwt* was 18.3 months compared to 37.8 months for the *IDHmut* patients, similar to GBM (18.4 months).

3.4. MRI features and mutation status

The univariate descriptive analysis of the difference between *IDHwt* and *IDHmut*, highlighted 8 of the VASARI features: f1 location, f3 eloquent brain, f9 multifocal, f10 T1/FLAIR ratio, f13 definition of nonenhancing margin, f20 cortical, f21 deep white matter invasion and f24 satellites (Table 1). *IDHwt* tumours were more likely to demonstrate a lower T1/FLAIR ratio (27/52) compared to 9 of 68 *IDHmut* astrocytomas, suggestive of an infiltrative rather than expansive pattern. The definition of the non-enhancing margin was poorly defined in 40 of 52

IDHwt astrocytomas compared to 28 of 68 *IDHmut* tumours. A higher proportion of *IDHwt* tumours demonstrated deep white matter invasion (30 of 52 (6 brainstem, 9 corpus callosum, 15 internal capsule) compared to 16 of 68 *IDHmut* astrocytomas).

IDHwt astrocytomas were more likely to be multifocal (9 of 52) or demonstrate a gliomatosis pattern (11 of 52) compared with 2 of 68 multifocal and 8 of 68 gliomatosis in the *IDHmut* reference set. There was a difference in tumour location between *IDHwt* and *IDHmut* tumours. The most common anatomical location for *IDHwt* tumours was the temporal lobe (15 of 52) whereas the frontal lobe was the most frequently involved site in *IDHmut* tumours. A higher proportion of *IDHwt* tumours were located in the thalamus (11 of 52) whereas the thalamus was not involved in any of the *IDHmut* cases. A higher proportion of *IDHwt* tumours involved eloquent brain, specifically speech receptive: (11 of 52 *IDHwt* compared to 2 of 68 *IDHmut*).

There were no significant differences in any of the MRI features describing contrast enhancement between *IDHwt* and *IDHmut* astrocytomas. 24 of the 52 *IDHwt* tumours and 36/68 *IDHmut* astrocytomas demonstrated no enhancement, whereas all the GBM cases demonstrated enhancement. Where enhancement was present, it was more likely to be patchy in the *IDHwt* astrocytomas (13 of 27) similar to the *IDHmut* reference set (20 of 30) whereas the GBM cases were more likely to be thick/nodular (7 of 13).

There were also no significant difference observed in diffusion characteristics between the *IDHwt* and *IDHmut* astrocytomas with the majority of lesions demonstrating facilitated diffusion (27/52 *IDHwt* and 37/68 *IDHmut*) rather than restricted diffusion. The GBM cases were more likely to demonstrate mixed diffusion with 3 cases demonstrating restricted diffusion.

3.5. Predicting mutation status from imaging features

Our Bayesian logistic regression model was used to estimate the odds ratios for each demographic and imaging feature within a probabilistic multivariable inferential framework. These ratios, ranked by strength of association, are shown in Fig. 3. In agreement with the univariate analysis, only a subset of the features were strongly associated with *IDH* mutation status. To quantify the optimal number of features to incorporate in a model with potential clinical predictive utility, we evaluated a set of 50 models with increasing numbers of independent variables, entered in order of their rank. The cross-validated performance of these models is shown in Fig. 4. Note that excellent performance (AUC = 0.92 \pm 0.07; balanced accuracy 0.81 \pm 0.09) was achieved with only the top five variables: age at presentation (OR = 0.94 \pm 0.03), tumour location within the thalamus (OR = 0.15 \pm 0.25), involvement of speech receptive areas (OR = 0.21 \pm 0.26), deep white matter invasion of the brainstem (OR = 0.10 \pm 0.32), and T1/FLAIR signal ratio (OR = 1.63 \pm 0.64).

An ROC curve for this five variable model is shown in Fig. 4. At the optimal decision threshold, this corresponds to a sensitivity of 0.83 and specificity of 0.85.

4. Discussion

In this comprehensive analysis of *IDHwt* and *IDHmut* WHO Grade II/III astrocytomas, we have shown that *IDHwt* have a survival equivalent to that of GBM, and much less than *IDHmut* astrocytomas, irrespective of histological grade. We have identified five most strongly predictive variables of *IDH* mutation status, and demonstrated—within a Bayesian framework that allows us to make this inference positively—that other imaging features are not contributory. A model based on these five features: older age at presentation, tumour location within the thalamus, involvement of speech receptive areas, deep white matter involvement of the brainstem and lower T1/FLAIR ratio shows excellent predictive performance for *IDHwt* astrocytomas, potentially alerting the clinician to *IDHwt* status and consequently earlier more

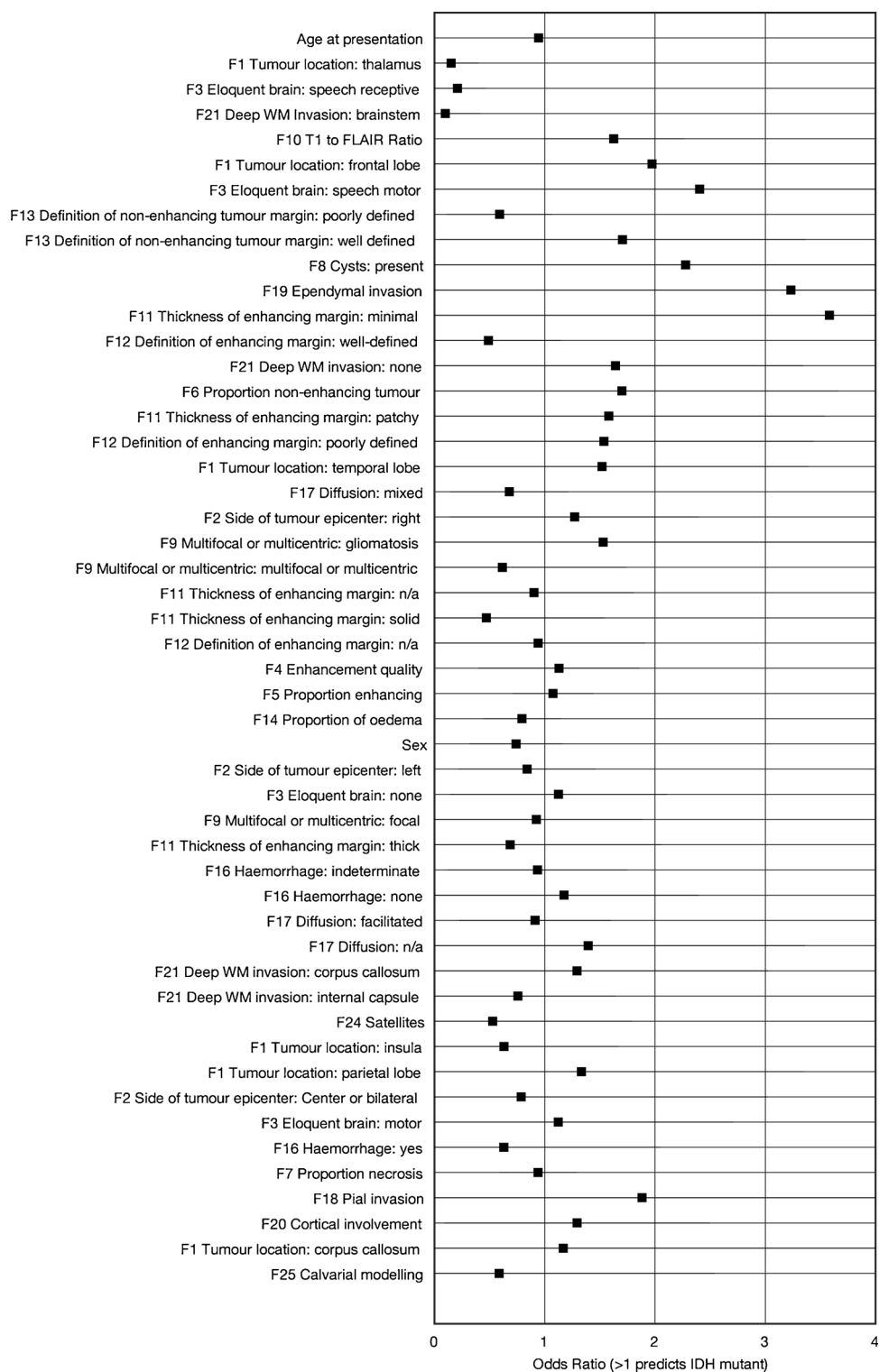


Fig. 3. Odds ratios of IDH status predictive demographic and VASARI features. legend: Forest plot of the odds ratio of demographic and VASARI features predictive of IDH mutation status, reparameterised to enable multivariable modelling within a Bayesian penalized logistic regression model. The features are ranked in order of decreasing strength of association. The black squares indicated the estimated mean, with their associated lines indicating ± 1 standard deviation of the parameter.

aggressive management.

The revised WHO classification of gliomas [1] has provided an opportunity to re-examine the imaging features of these tumours with potential for additional validation and potential for an imaging-based classification that could complement the genomic classification. This would be particularly useful in unresectable tumours where a policy of surveillance may be preferred without recourse to a histological and

molecular diagnosis. Our study findings of a more invasive imaging phenotype in *IDHwt* astrocytomas is supported by a recent radiogenomic study of 110 WHO grade II and III astrocytomas from The Cancer Genome Atlas [7], reporting that the 25 *IDHwt* tumours were more likely to be associated with an irregular tumour boundary and a poorer outcome. The authors used a computer algorithm approach to analyze tumour shape in two or three dimensions and hypothesized that

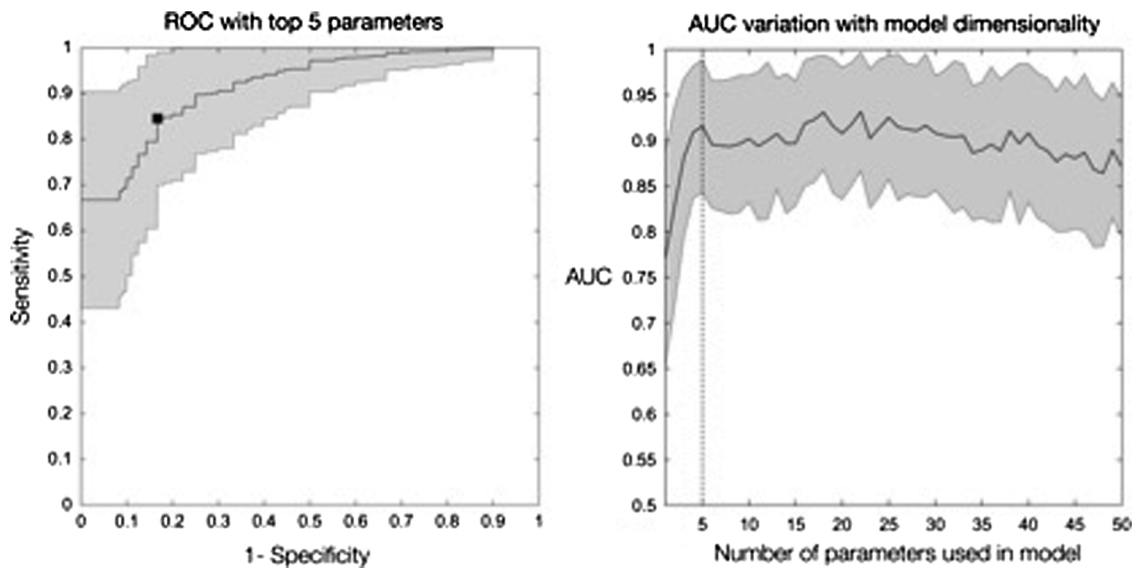


Fig. 4. Predicting IDH mutation status from demographic and VASARI features. legend: The plot on the right shows the estimated AUC (black line) tested on a held out random sample of 15% of the dataset with logistic regression models incorporating incrementally larger number of features, from 1 to 50, added in order of the rank displayed in Fig. 3. The grey lines indicate ± 1 standard deviation of the parameter, estimated by running each model with randomly resampled training and testing data 50 times. Note that there is no substantial increase in performance beyond the top five features. The plot on the left shows the receiver operating characteristic (ROC) curve for the 5 parameter model, with ± 1 standard deviation given in grey. The black square shows the optimal decision point. Note excellent predictive performance.

the irregular tumour boundary corresponded to an “invasive” phenotype. In another study of 198 diffuse low grade gliomas, the 34 *IDHwt* astrocytomas were more likely to have an indistinct tumour margin [8]. The authors also reported an association with anatomical location, similar to our findings, where *IDHwt* astrocytomas were more likely to be temporo-insular lesions compared to the more frequently observed frontal location in *IDHmut* astrocytomas. The temporo-insular predominance of *IDHwt* astrocytomas corresponds to the increased involvement of eloquent brain observed in our study with the speech receptive area being most affected.

We also observed an increased incidence of thalamic involvement in the *IDHwt* tumours, seen in 11 of the 52 (21.1%) *IDHwt* astrocytomas compared to no thalamic involvement in any of the 68 *IDHmut* astrocytomas and 3 of the 26 (11.5%) GBM tumours. A recent study of 331 gliomas reported an incidence of 6.4% in the deep structures of the cerebrum but did not investigate anatomical location according to *IDH* mutation status [9]. Our findings, not previously reported in the literature, may be due to institutional bias of increased referrals for complex inoperable tumours. Nevertheless, our findings suggest that thalamic involvement is more likely to be seen in *IDHwt* astrocytomas and should be referred for early biopsy.

The importance of the T1/FLAIR ratio is an interesting finding in our study. It is well-established in high grade gliomas that the surrounding nonenhancing region represented by T2W and FLAIR signal abnormality is a mixture of infiltrative tumour and oedema [10]. In GBM, multiple studies investigating the qualitative extent of peritumoural oedema/nonenhancing disease have shown that the presence and extent of FLAIR signal abnormality is a negative prognostic factor [11–13] with increased resection of FLAIR abnormalities correlating positively with progression-free survival [14]. The inclusion of FLAIR assessment in the recently updated RANO criteria also highlights the importance of FLAIR signal in monitoring treatment response [15]. Whilst recent reports have described an ill-defined border on FLAIR sequences predictive of *IDHwt* tumours [3,16,17] to our knowledge, there are no reports of T1/FLAIR ratio assessment in low-grade gliomas. This MR descriptor offers potential as an important prognosticator in these predominantly non-enhancing tumours.

Our patient survival data supports the growing literature that *IDHwt*

grade II/III astrocytomas have a poorer survival than their *IDHmut* equivalents [18,19]. The TCGA study of 31 *IDHwt* grade II/III astrocytomas found an intermediate overall survival between *IDHmut* grade II/III and GBM as we have shown here [20]. As seen in our study, WHO grade had a significant influence on survival. Whilst survival was more similar to GBM than *IDHmut*, our *IDHwt* reference set was radiologically more similar to the *IDHmut* astrocytomas than GBM: less likely to show enhancement, macroscopic necrosis and haemorrhage. In particular, the majority of *IDHwt* and *IDHmut* tumours were non-enhancing and where enhancement was present, tended to be patchy rather than thick/nodular or solid, as seen in GBMs.

It is well established that diffusion can support glioma grading and survival prediction in GBM and diffuse gliomas [21–23]. A recent study of 65 WHO grade II and III astrocytomas demonstrated a lower ADC in *IDHwt* astrocytomas compared to *IDHmut* [24]. However, we were unable to detect a significant difference in diffusion characteristics between *IDHwt* and *IDHmut* astrocytomas. The absence of an available ADC map in 22 patients may have limited our power to detect significant differences. Low inter-rater agreements may have been due to T2 effects and attempting to describe heterogeneous diffusion appearances within the predefined VASARI diffusion categories.

Radiologist-made measurements are potentially open to user bias. In this study the neuroradiologists were blinded to *IDH* mutation status and histopathological grade and where agreement was poor, a consensus review was performed. Studies building radiogenomic maps using quantitative features have shown that these may be a useful complementary strategy to non invasive GBM management [25]. Such studies are currently underway at our institution and we expect the preliminary findings in this study to be validated in a larger dataset.

5. Conclusion

Our results provide further evidence that *IDHwt* astrocytomas demonstrate poorer survival, more equivalent to that for GBM, than *IDHmut* astrocytomas. These tumours are more likely to be located in eloquent areas, show deep white matter invasion and demonstrate more infiltrative radiological features with lower T1/FLAIR ratio when compared to their *IDHmut* counterparts.

We believe that these findings may help clinicians to predict *IDH* mutation status on imaging, identifying those patients that are more likely to have an *IDHwt* tumour for early biopsy/resection and more GBM-like treatment. This could have important implications for diagnostic decision-making, by alerting clinicians to the presence of early stage glioblastoma.

Disclosures

No author disclosures.

Conflict of interest

None.

Acknowledgments

This study was undertaken at University College London Hospitals/ University College London which received a proportion of funding from the National Institute of Health Research Biomedical Research Centre. PN is funded by the Wellcome Trust, the Department of Health, and the NIHR UCLH BRC.

References

- [1] D.N. Louis, A. Perry, G. Reifenberger, et al., The 2016 World Health Organization classification of tumors of the central nervous system: a summary, *Acta Neuropathol.* (131) (2016) 803–820.
- [2] D.E. Reuss, A. Kratz, F. Sahm, et al., Adult *IDH* wild type astrocytomas biologically and clinically resolve into other tumor entities, *Acta Neuropathol.* 130 (2015) 407–417.
- [3] R.L. Delfanti, D.E. Piccioni, J. Handwerker, et al., Imaging correlates for the 2016 update on WHO classification of grade II/III gliomas: implications for *IDH*, *1p/19q* and *ATRX* status, *J. Neurooncol.* (135) (2017) 601–609.
- [4] W. Tan, J. Xiong, W. Huang, et al., Noninvasively detecting Isocitrate dehydrogenase 1 gene status in astrocytoma by dynamic susceptibility contrast MRI, *J. Magn. Reson. Imaging* 45 (2017) 492–499.
- [5] M.A. Mazuwowski, A. Desjardins, J.M. Malof, Imaging descriptors improve the predictive power of survival models for glioblastoma patients, *Neuro Oncol.* 15 (2013) 1389–1394.
- [6] D.E. Reuss, A. Kratz, F. Sahm, et al., Adult *IDH* wild type astrocytomas biologically and clinically resolve into other tumor entities, *Acta Neuropathol.* 130 (2015) 407–417.
- [7] M.A. Mazuwowski, K. Clark, N.M. Czarnek, et al., Radiogenomics of lower-grade glioma: algorithmically-assessed tumor shape is associated with tumor genomic subtypes and patient outcomes in a multi-institutional study with the cancer genome Atlas data, *J. Neurooncol.* 133 (2017) 27–35.
- [8] A. Darlix, J. Deverdun, C.N. Menjot de, et al., *IDH* mutation and *1p19q* codeletion distinguish two radiological patterns of diffuse low-grade gliomas, *J. Neurooncol.* 133 (2017) 37–45.
- [9] S. Larjavaara, R. Mantyla, T. Salminen, et al., Incidence of gliomas by anatomic location, *Neuro Oncol.* 9 (2007) 319–325.
- [10] A.T. Parsa, S. Wachhorst, K.R. Lamborn, et al., Prognostic significance of intracranial dissemination of glioblastoma multiforme in adults, *J. Neurosurg.* 102 (2005) 622–628.
- [11] M.A. Hammoud, R. Sawaya, W. Shi, et al., Prognostic significance of preoperative MRI scans in glioblastoma multiforme, *J. Neurooncol.* 27 (1996) 65–73.
- [12] W.B. Pope, J. Sayre, A. Perlina, et al., MR imaging correlates of survival in patients with high-grade gliomas, *AJNR Am. J. Neuroradiol.* 26 (2005) 2466–2474.
- [13] K. Schoenegger, S. Oberndorfer, B. Wuschitz, et al., Peritumoral edema on MRI at initial diagnosis: an independent prognostic factor for glioblastoma? *Eur. J. Neurol.* 16 (2009) 874–878.
- [14] J.L. Yan, A. van der Hoorn, T.J. Larkin, et al., Extent of resection of peritumoral diffusion tensor imaging-detected abnormality as a predictor of survival in adult glioblastoma patients, *J. Neurosurg.* 126 (2017) 234–241.
- [15] P.Y. Wen, D.R. Macdonald, D.A. Reardon, et al., Updated response assessment criteria for high-grade gliomas: response assessment in neuro-oncology working group, *J. Clin. Oncol.* 28 (2010) 1963–1972.
- [16] B. Zhang, K. Chang, S. Ramkissoon, et al., Multimodal MRI features predict isocitrate dehydrogenase genotype in high-grade gliomas, *Neuro Oncol.* 19 (2017) 109–117.
- [17] H. Zhou, M. Vallieres, H.X. Bai, et al., MRI features predict survival and molecular markers in diffuse lower-grade gliomas, *Neuro Oncol.* 19 (2017) 862–870.
- [18] Y. Suzuki, K. Shirai, K. Oka, et al., Higher pAkt expression predicts a significant worse prognosis in glioblastomas, *J. Radiat. Res.* 51 (2010) 343–348.
- [19] C. Hartmann, B. Hentschel, W. Wick, et al., Patients with *IDH1* wild type anaplastic astrocytomas exhibit worse prognosis than *IDH1*-mutated glioblastomas, and *IDH1* mutation status accounts for the unfavorable prognostic effect of higher age: implications for classification of gliomas, *Acta Neuropathol.* 120 (2010) 707–718.
- [20] The Cancer Genome Atlas Research Network, Comprehensive, integrative genomic analysis of diffuse lower-grade gliomas, *N. Engl. J. Med.* 372 (2015) 2481–2498.
- [21] W.B. Pope, X.J. Qiao, H.J. Kim, et al., Apparent diffusion coefficient histogram analysis stratifies progression-free and overall survival in patients with recurrent GBM treated with bevacizumab: a multi-center study, *J. Neurooncol.* 108 (2012) 491–498.
- [22] W.B. Pope, H.J. Kim, J. Huo, et al., Recurrent glioblastoma multiforme: ADC histogram analysis predicts response to bevacizumab treatment, *Radiology* 252 (2009) 182–189.
- [23] A. Hilario, J.M. Sepulveda, A. Perez-Nunez, et al., A prognostic model based on preoperative MRI predicts overall survival in patients with diffuse gliomas, *AJNR Am. J. Neuroradiol.* 35 (2014) 1096–1102.
- [24] K. Leu, G.A. Ott, A. Lai, et al., Perfusion and diffusion MRI signatures in histologic and genetic subtypes of WHO grade II-III diffuse gliomas, *J. Neurooncol.* (2017).
- [25] O. Gevaert, L.A. Mitchell, A.S. Achrol, et al., Glioblastoma multiforme: exploratory radiogenomic analysis by using quantitative image features, *Radiology* 273 (2014) 168–174.